

Transverse asymmetry of ${}^3\vec{\text{He}}$ and the magnetic form factor of the neutron

A. Kievsky¹, E. Pace², and G. Salmè³

¹ Istituto Nazionale di Fisica Nucleare, Sezione di Pisa, Via Buonarroti 2, I-56100 Pisa, Italy

² Dipartimento di Fisica, Università di Roma “Tor Vergata” and Istituto Nazionale di Fisica Nucleare, Sezione Tor Vergata, Via della Ricerca Scientifica 1, I-00133 Roma, Italy

³ Istituto Nazionale di Fisica Nucleare, Sezione Roma I, P. le A. Moro 2, I-00185 Roma, Italy

Received: 3 Oct 2003 / Accepted: 14 Nov 2003 /

Published Online: 6 Feb 2004 – © Società Italiana di Fisica / Springer-Verlag 2004

Abstract. Preliminary calculations of the inclusive electromagnetic responses by a polarized ${}^3\text{He}$ target, including final state interaction effects, relativistic kinematics and a relativistic electron-nucleon cross section, are presented. The features of our approach will be briefly illustrated, in order to yield an insight on the model dependence affecting the extraction of the neutron magnetic form factor, G_M^n , from the inclusive scattering of polarized electrons by a polarized ${}^3\text{He}$ target, recently explored at TJLAB for $0.1 (GeV/c)^2 \leq Q^2 \leq 0.6 (GeV/c)^2$.

PACS. 13.40Gp, – 13.60.Hb – 21.45+v – 24.70.+s

1 Introduction

In the last few years, an impressive amount of experimental work (see, for a recent review, K. de Jager [1]) has been devoted to an accurate investigation of nucleon electromagnetic (em) form factors, obtaining unexpected results like the puzzling ratio G_E/G_M for the proton (see, e.g., [2]). In order to have a complete knowledge of the nucleon form factors, one has to face with the particularly difficult problem represented by the extraction of the neutron em form factors, since free neutron targets do not exist in nature. To overcome such a difficulty, light nuclei, such as deuteron or polarized ${}^3\text{He}$, have been considered as an effective neutron target. As a matter of fact, within a naive model for a polarized ${}^3\text{He}$ target with only a symmetric S-wave component in the bound-state, the two protons have opposite spins and therefore only the neutron spin contributes to the em polarized responses of the target. Within a realistic description of ${}^3\text{He}$, it is not a trivial task to disentangle the neutron information from the nuclear-structure effects, given the many effects playing relevant roles, like: i) the “small” components of the bound-state wave function; ii) the Δ excitation; iii) the inclusion of the final state interaction (FSI), between the knocked-out nucleon and the interacting spectator pair; iv) the meson exchange currents (MEC); v) the relativistic corrections. As a first step, the analysis of inclusive responses of polarized ${}^3\text{He}$ was carried out within the *plane wave impulse approximation* (PWIA) in [3,4,5,6], where realistic nucleon-nucleon interactions were adopted and in

the final state only the interaction between the spectator pair and the knocked-out nucleon was disregarded. Moreover a relativistic electron-nucleon cross section [7] was adopted.

Recently, a step forward has been performed through calculations of the em responses which include FSI, but within a non relativistic framework [8,9].

In this contribution, a review of recent applications of our PWIA description of the polarized responses will be given, along with a presentation of preliminary calculations which include FSI in the two-body break-up channel.

In Sect. 2 the polarized cross section in PWIA will be briefly reviewed and relevant applications will be presented; in Sect. 3 the fully-interacting wave function for a three-nucleon system in the continuous spectrum will be introduced; in Sect. 4, preliminary results with FSI for the transverse response of a polarized ${}^3\text{He}$ target will be shown; Sect. 5 contains summary and perspectives.

2 The polarized cross section in PWIA

The inclusive scattering of polarized electrons (with helicity h) by a polarized ${}^3\text{He}$ target ($\vec{e} + {}^3\vec{\text{He}} \rightarrow e' + X$) is given by

$$\frac{d^2\sigma(h)}{d\Omega_2 dw} = \Sigma + h \Delta \quad (1)$$

with

$$\Sigma = \sigma_{Mott} \left[\left(\frac{Q^2}{|\mathbf{q}|^2} \right)^2 A_L(Q^2, \omega) + \left(\frac{Q^2}{2|\mathbf{q}|^2} + \tan^2 \frac{\theta_e}{2} \right) A_T(Q^2, \omega) \right] \quad (2)$$

$$\Delta = -\sigma_{Mott} \tan \frac{\theta_e}{2} \times \left\{ \cos \theta^* A_{T'}(Q^2, \omega) \frac{(\epsilon_i + \epsilon_f)}{|\mathbf{q}|} \tan \frac{\theta_e}{2} + -\frac{Q^2}{|\mathbf{q}|^2 \sqrt{2}} \sin \theta^* \cos \phi^* A_{TL'}(Q^2, \omega) \right\} \quad (3)$$

where θ_e is the scattering angle, $\epsilon_{i(f)}$ the energy of the initial (final) electron, θ^* and ϕ^* are the azimuthal and polar angles of the target polarization vector, with respect to the direction of the three-momentum transfer \mathbf{q} ; $Q^2 = |\mathbf{q}|^2 - \omega^2$, with ω the energy transfer. The unpolarized (A_L , A_T) and polarized ($A_{T'}$, $A_{TL'}$) inclusive responses contain the nuclear-structure effects. The key point in our PWIA calculation of the inclusive responses is the following approximation of the three-nucleon wave function describing the final state, viz.

$$|j, j_z, T, T_z, \pi, \epsilon_{int}, \alpha; \mathbf{P}\rangle \rightarrow \frac{1}{\sqrt{3}} \times |\mathbf{p}_f, \sigma_f \tau_f\rangle |j_{23} m_{23}, T_{23} \tau_{23}, \pi_{23}, \lambda_{23}, \epsilon_{23}; \mathbf{P}_{23}\rangle \quad (4)$$

with $j(j_z)$ the total angular momentum (third component), $T(T_z)$ the total isospin (third component), π the total parity, ϵ_{int} the intrinsic energy of the three-nucleon system, $\alpha \equiv \{j_{23} T_{23} \lambda_{23}, \pi_{23}, \epsilon_{23}\}$, $\mathbf{P} = \mathbf{p}_f + \mathbf{P}_{23}$ the three-momentum of the three-nucleon centre of mass (CM), $|\mathbf{p}_f, \sigma_f \tau_f\rangle$ the plane wave describing the knocked-out nucleon. In (4), the wave function of the fully-interacting spectator pair is given by $|j_{23} m_{23}, T_{23} \tau_{23}, \pi_{23}, \epsilon_{23}; \mathbf{P}_{23}\rangle$. The other terms, that properly antisymmetrize the approximated three-nucleon wave function, are dropped out, since only the direct interaction between the virtual photon and the struck nucleon is taken into account.

Following [4], the nuclear response functions can be expressed through a 2x2 matrix, $\hat{\mathbf{P}}_{\mathcal{M}}^N(\mathbf{p}, E)$, representing the spin dependent spectral function of a nucleon, N , inside a nucleus with component of the total angular momentum along the polarization \mathbf{S}_A equal to \mathcal{M} . The elements of the matrix $\hat{\mathbf{P}}_{\mathcal{M}}^N(\mathbf{p}, E)$ are given by

$$P_{\sigma, \sigma', \mathcal{M}}^N(\mathbf{p}, E) = \sum_{f(A-1)} N \langle \mathbf{p}, \sigma; \psi_{f(A-1)} | \psi_{j\mathcal{M}} \rangle \langle \psi_{j\mathcal{M}} | \psi_{f(A-1)}; \mathbf{p}, \sigma' \rangle_N \delta(E - E_{f(A-1)} + E_A) \quad (5)$$

where E and \mathbf{p} are the missing energy and the three-momentum of the nucleon in the bound state, respectively, $|\psi_{j\mathcal{M}}\rangle$ is the ground state of the target nucleus with polarization \mathbf{S}_A , and $|\psi_{f(A-1)}; \mathbf{p}, \sigma'\rangle_N$ a shorthand

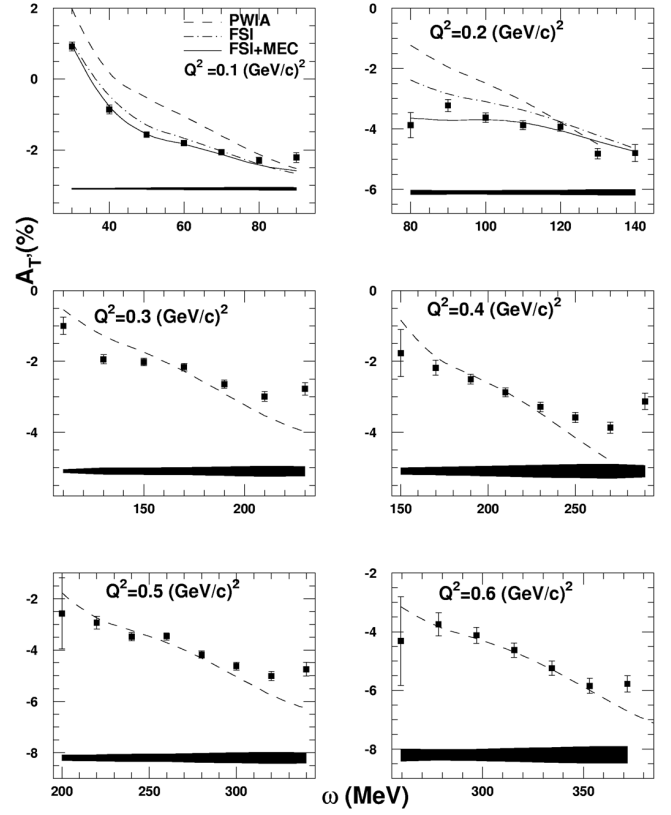


Fig. 1. The transverse asymmetry $A_{T'}$ vs the energy transfer, ω , for different values of Q^2 . Dashed lines: PWIA calculations within our approach [5]; dash-dotted lines and solid lines: Faddeev calculations with FSI only and with FSI + MEC, respectively [8,9]. (After W. Xu et al. [10])

notation for the *plane wave impulse* approximation of a three-nucleon system in the continuum, given by (4). For $j = 1/2$, $\hat{\mathbf{P}}_{\mathcal{M}}^N(\mathbf{p}, E)$ can be written in a more compact form as follows [4]

$$\hat{\mathbf{P}}_{\mathcal{M}}^N(\mathbf{p}, E) = \frac{1}{2} \left\{ B_{0, \mathcal{M}}^N(|\mathbf{p}|, E) + \sigma \cdot [\mathbf{S}_A B_{1, \mathcal{M}}^N(|\mathbf{p}|, E) + \hat{p} (\hat{p} \cdot \mathbf{S}_A) B_{2, \mathcal{M}}^N(|\mathbf{p}|, E)] \right\} \quad (6)$$

where $B_{0, \mathcal{M}}^N(|\mathbf{p}|, E)$ is the trace of $\hat{\mathbf{P}}_{\mathcal{M}}^N(\mathbf{p}, E)$ and is the usual unpolarized spectral function, while the other two functions, $B_{1, \mathcal{M}}^N(|\mathbf{p}|, E)$ and $B_{2, \mathcal{M}}^N(|\mathbf{p}|, E)$, describe the spin structure of the probability distribution of finding a nucleon in the nucleus with a given momentum, missing energy and polarization. Then, the calculation of the inclusive responses in (2) and (3) proceeds through the evaluation of the functions $B_{i, \mathcal{M}}^N$ [3,4]. It should be pointed out that, in our PWIA, we take into account relativistic effects, like the relativistic treatment of the final state kinematics and the relativistic electron-nucleon cross section CC1 proposed in [7]. In Figs. 1 and 2 calculations of the transverse (polarized) response $A_{T'}$, obtained with the AV18 nucleon-nucleon potential [11], are compared with the data recently measured at TJLAB, both in the region of the quasielastic peak (Fig. 1) and in the low

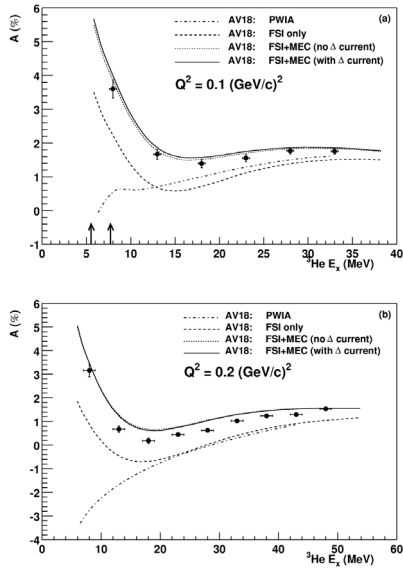


Fig. 2. The transverse asymmetry $A_{T'}$ vs $E_X = \sqrt{M_{He}^2 + 2M_{He}\omega - Q^2} - M_{He}$ (in the non relativistic limit $E_X = \epsilon_{int} + B_{He}$). *Dash-dotted lines:* our PWIA calculations [5]; *dashed and solid lines:* FSI and FSI + MEC calculations [8,9], respectively. Experimental data belong to a kinematical region where the energy transfer is lower than the value corresponding to the quasielastic peak (after F. Xiong et al. [14])

energy-transfer region (Fig. 2). At low values of Q^2 , calculations [8,9] including FSI and MEC, but within a non relativistic approach, are also shown. On one side, the disagreement, at low Q^2 , between our PWIA calculations [5] and both experimental data and calculations including FSI illustrates the relevance of nuclear-structure effects beyond PWIA. On the other side, at higher values of Q^2 , in the region close to the quasielastic peak, the quite reasonable description of the data achieved by our PWIA (that contains relativistic effects) confirms the physical expectation of a minor role played by FSI, when the nucleon rapidly gets out. Experimental data in the region of the quasielastic peak and theoretical results (necessary for an estimate of the model dependence of the procedure) have been exploited for extracting the neutron form factor, $G_M^n(Q^2)$ in the range $0.1 \leq Q^2 \leq 0.6$ (GeV/c) 2 , see Fig. 3. For $Q^2 \leq 0.2$ (GeV/c) 2 (diamonds) the calculations by the Bochum group [8,9] were used, while for $Q^2 > 0.2$ (GeV/c) 2 our PWIA calculations have been employed in the procedure of extraction [13] (full dots). At the quasielastic peak, the uncertainties due to FSI and MEC, estimated from the calculations of the Bochum group, amount to few percent for $Q^2 > 0.2$ (GeV/c) 2 , see W. Xu et al. [13].

3 Three-nucleon scattering states

The fully-interacting, intrinsic wave function, for a three-nucleon system in the continuous spectrum, can be de-

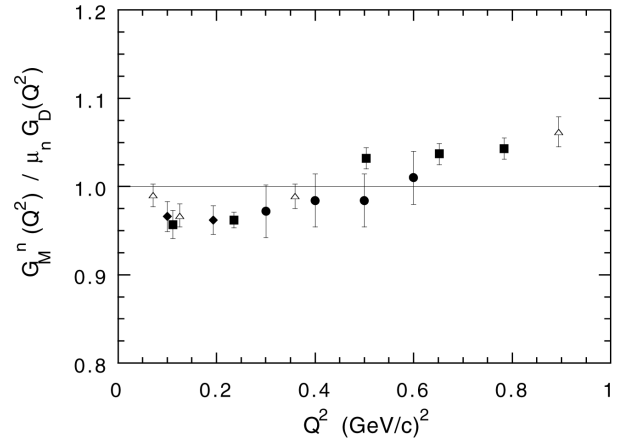


Fig. 3. The most recent experimental determinations of $G_M^n/\mu_n G_D$ vs Q^2 ($G_D = (1 + Q^2/0.71)^{-2}$). *Triangles:* G. Kubon et al. [15]; *diamonds:* W. Xu et al. [10]; *black squares:* H. Anklin et al. [12]; *full dots:* W. Xu et al. [13]. The full dots have been extracted [13] using our PWIA calculations [5]

composed [16] as follows

$$\begin{aligned} \Phi^{jj_z TT_z \pi} &= \Psi_A^{jj_z TT_z \pi} + \Psi_C^{jj_z TT_z \pi} = \\ &= \sum_{i=3} \left[\psi_A^{jj_z TT_z \pi}(i) + \psi_C^{jj_z TT_z \pi}(i) \right] \end{aligned} \quad (7)$$

where the intrinsic energy is understood; $\Psi_A^{jj_z TT_z \pi}$ is the solution of the Schrödinger equation in the asymptotic region, with two well separated clusters, $\Psi_C^{jj_z TT_z \pi}$ describes the system when the three nucleons are close each other. The functions $\psi_A^{jj_z TT_z \pi}(i)$ and $\psi_C^{jj_z TT_z \pi}(i)$ are Faddeev-like amplitudes, corresponding to the three permutations of the intrinsic coordinates ($\equiv \{\mathbf{r}_1, \mathbf{r}_2, \mathbf{r}_3\}$).

The asymptotic component, $\Psi_A^{jj_z TT_z \pi}$, can be recast in a different way, in order to emphasize its physical content. If one considers the case of a N-d scattering state, for the sake of concreteness, one has

$$\begin{aligned} \Psi_A^{LX jj_z TT_z \pi} &= \Omega_{LXj}^R(\mathbf{x}_1, \mathbf{y}_1) + \\ &+ \sum_{L'X'}^j \mathcal{L}_{LL'}^{XX'} \left[\iota \Omega_{L'X'j}^R(\mathbf{x}_1, \mathbf{y}_1) + \Omega_{L'X'j}^I(\mathbf{x}_1, \mathbf{y}_1) \right] + \\ &+ \left[\psi_A^{LX jj_z TT_z}(2) + \psi_A^{LX jj_z TT_z}(3) \right] \end{aligned} \quad (8)$$

where L is the relative orbital angular momentum of N with respect to the deuteron, X is the intermediate coupling of the spin of the nucleon with the total angular momentum of the deuteron, and the intrinsic coordinates $\{\mathbf{x}_1, \mathbf{y}_1\}$ are defined as follows

$$\mathbf{x}_1 = \mathbf{r}_2 - \mathbf{r}_3 \quad \mathbf{y}_1 = \frac{1}{\sqrt{3}} [\mathbf{r}_2 + \mathbf{r}_3 - 2\mathbf{r}_1]. \quad (9)$$

In (8), $\Omega_{LXj}^{R(I)}$ represents the regular ("irregular", but properly regularized at small distances [16,17]) solution describing the free scattering of a nucleon by an interacting pair (in this case a deuteron); the matrix \mathcal{L} is given by

$$\mathcal{L} = \frac{S - 1}{2\iota} = -\pi\mathcal{T} \quad (10)$$

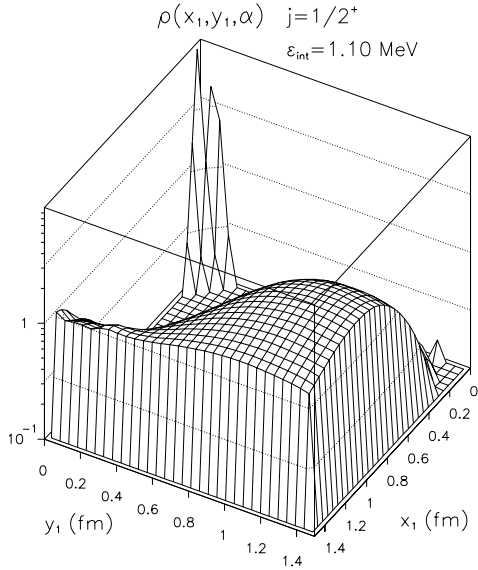


Fig. 4. The density function defined in (13) vs the two Jacobi coordinates, $\{|\mathbf{x}_1|, |\mathbf{y}_1|\}$ for $j = 1/2$, $T = 1/2$, $\pi = +1$ and $\epsilon_{int} = 1.1$ MeV

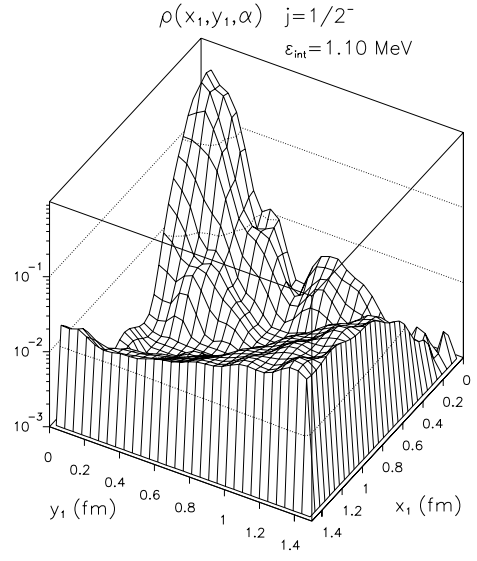


Fig. 5. The density function defined in (13) vs the two Jacobi coordinates, $\{|\mathbf{x}_1|, |\mathbf{y}_1|\}$ for $j = 1/2$, $T = 1/2$, $\pi = -1$ and $\epsilon_{int} = 1.1$ MeV

with \mathcal{S} and \mathcal{T} the S-matrix and the T-matrix, respectively. Similar expressions hold for $\psi_A^{LXjj_zTT_z}(2)$ and $\psi_A^{LXjj_zTT_z}(3)$. Three terms can be recognized in (8):

- the first one produces the PWIA, i.e. contains an interacting pair and a free particle;
- the second term describes the rescattering between the interacting pair and the asymptotically free particle;
- the third term, $\left[\psi_A^{LXjj_zTT_z}(2) + \psi_A^{LXjj_zTT_z}(3)\right]$, takes care of the correct antisymmetrization of $\Psi_C^{jj_zTT_z\pi}$.

The core component, $\Psi_C^{jj_zTT_z\pi}$, goes to zero for large interparticle distances and energies below the deuteron breakup threshold, while for higher energies, must reproduce a three outgoing particle state. In the approach developed in [16], $\Psi_C^{jj_zTT_z\pi}$ is explicitly written as an expansion on a basis of Hyperspherical Harmonics Polynomials, with the inclusion of pair-correlation functions, to be determined along with the elements of the S-matrix (see (10)), through a variational procedure (complex Kohn variational principle).

In the coordinate space the state (7) can be written

$$\langle \mathbf{y}_1, \mathbf{x}_1 | j, j_z; TT_z, \pi, \epsilon_{int}; \beta \rangle = \frac{1}{\sqrt{3}} \sum_{L'X'} \sum_{j'_{23}S'_{23}} \sum_{\ell} \mathcal{Y}_{L'X'j'_{23}TT_z}^{j'_{23}S'_{23}\ell}(\hat{x}_1, \hat{y}_1) \mathcal{J}_{L'X'j'T}^{j'_{23}S'_{23}\ell}(|\mathbf{y}_1|, |\mathbf{x}_1|, \epsilon_{int}; \beta) \quad (11)$$

where $\beta \equiv \{\alpha; LX\}$ is the set of quantum numbers of the incoming wave. The “trivial” dependence upon angular, spin and isospin variables is described by the functions

$$\mathcal{Y}_{L'X'j'_{23}TT_z}^{j'_{23}S'_{23}\ell}(\hat{x}_1, \hat{y}_1) = \sum_{M\sigma} \sum_{M_X m_{23}} \langle j'_{23} m_{23} \frac{1}{2} \sigma | X' M_X \rangle \chi_{\frac{1}{2}}^{\sigma} \langle X' M_X, L' M' | j j_z \rangle Y_{L'M'}(\Omega_{\hat{y}_1}) \sum_m \sum_{m_{S'_{23}}} \chi_{S'_{23}}^{m_{S'_{23}}} Y_{\ell m}(\Omega_{\hat{x}_1})$$

$$\langle \ell m S'_{23} m_{S'_{23}} | j'_{23} m'_{23} \rangle \sum_{\tau' \tau'_{23}} \langle T'_{23} \tau'_{23} \frac{1}{2} \tau' | TT_z \rangle \mathcal{T}_{\frac{1}{2}}^{\tau'} \mathcal{T}_{T'_{23}}^{\tau'_{23}} \quad (12)$$

that form a complete basis for a two-fermion system (T'_{23} is determined through the parity of S'_{23} and ℓ), while the “non trivial” structure of the final state wave function is described by $\mathcal{J}_{L'X'j'T}^{j'_{23}S'_{23}\ell}(|\mathbf{y}_1|, |\mathbf{x}_1|, \epsilon_{int}; \beta)$. In order to give an insight on the three-nucleon wave function, it is useful to introduce density functions defined as follows

$$\begin{aligned} \rho(|\mathbf{y}_1|, |\mathbf{x}_1|, \alpha) &= \\ &= \sum_{LX} \sum_{L'X'} \sum_{j'_{23}S'_{23}} \sum_{\ell} \left\{ \left| \Re \left[\mathcal{J}_{L'X'j'T}^{j'_{23}S'_{23}\ell}(|\mathbf{y}_1|, |\mathbf{x}_1|, \epsilon_{int}; \beta) \right] \right|^2 + \right. \\ &\left. + \left| \Im \left[\mathcal{J}_{L'X'j'T}^{j'_{23}S'_{23}\ell}(|\mathbf{y}_1|, |\mathbf{x}_1|, \epsilon_{int}; \beta) \right] \right|^2 \right\} \quad (13) \end{aligned}$$

Such density functions yield information on the probability distribution of a nucleon in the final state, taking into account the caveat that the wave functions in the continuum are not square integrable. Examples of the density function for a state with an asymptotic $p + d$ cluster is presented in Figs. 4 and 5 for $j = 1/2^+$ and $j = 1/2^-$, respectively, with $\epsilon_{int} = 1.1$ MeV.

4 Beyond PWIA

In order to include the full interaction between the three nucleons in the final state, one has to abandon the elegant and compact language of the spectral functions, reverting to a lengthy calculation of matrix elements of the current operator of the three-body system. We approximate the current operator as a sum of one-body operators, i.e. we do not consider for the moment two-body contributions,

viz

$$\begin{aligned}
 & \langle j', j'_z; T', T'_z, \pi', \epsilon'_{int}; \beta'; \mathbf{q} | J_{IA}^\mu(0) | \frac{1}{2}, j_z; \frac{1}{2}, T_z, \pi_b, \epsilon_b; \mathbf{0} \rangle = \\
 & = 3 \sum_{\sigma_1} \sum_{\sigma'_1} \sum_{\sigma_2} \sum_{\sigma_3} \int d\mathbf{k}_1 d\mathbf{k}_2 \times \\
 & \langle j', j'_z; T', T'_z, \pi', \epsilon'_{int}; \beta | \mathbf{k}'_1, \mathbf{k}'_2, \sigma'_1, \sigma_2, \sigma_3 \rangle \times \\
 & \langle \mathbf{q} + \mathbf{k}_1, \sigma'_1 | J_{1,free}^\mu(0) | \mathbf{k}_1, \sigma_1 \rangle \times \\
 & \langle \mathbf{k}_1, \mathbf{k}_2, \sigma_1, \sigma_2, \sigma_3 | \frac{1}{2}, j_z; \frac{1}{2}, T_z, \pi_b, \epsilon_b \rangle
 \end{aligned} \quad (14)$$

where $\langle \mathbf{k}_1, \mathbf{k}_2, \sigma_1, \sigma_2, \sigma_3 | j, j_z; T, T_z, \pi, \epsilon \rangle$ indicates the intrinsic three-body wave function, related to the state containing the centre of mass motion by the following simplified expression

$$\begin{aligned}
 & \langle \mathbf{p}_1, \mathbf{p}_2, \mathbf{p}_3, \sigma_1, \sigma_2, \sigma_3 | j, j_z; T, T_z, \pi, \epsilon; \mathbf{P} \rangle = \\
 & \delta(\mathbf{p}_1 + \mathbf{p}_2 + \mathbf{p}_3 - \mathbf{P}) \times \\
 & \langle \mathbf{k}_1, \mathbf{k}_2, \sigma_1, \sigma_2, \sigma_3 | j, j_z; T, T_z, \pi, \epsilon \rangle
 \end{aligned} \quad (15)$$

where \mathbf{k}_i is the spatial part of the four-momentum $k_i^\mu \equiv \{\sqrt{m^2 + |\mathbf{k}_i|^2}, \mathbf{k}_i\} = B_\nu^\mu(\mathbf{P}/M)p_i^\mu$, with B_ν^μ the appropriate boost for the chosen Hamiltonian dynamics (see, e.g., [19]). The expression in (15) is an approximate one, since the Wigner functions corresponding to the boost transformations, as well as other kinematical factors, are dropped out in this introductory presentation of our approach. Our preliminary calculations based on the matrix elements of the em current of ${}^3\text{He}$, (14), both for the unpolarized (A_L and A_T) and the polarized ($A_{T'}$) responses are presented in Figs. 6,7,8 and 9. FSI is taken into account in the two-body break-up channel (where a fully interacting three-nucleon state behaves asymptotically like a pd system) for $j' \leq 5/2$, while PWIA is used in all other channels. The AV18 nucleon-nucleon interaction [11] has been adopted, without Coulomb effects nor three-body forces (included in the future). Comparisons with the experimental data and the PWIA calculations are also shown. The strong effect of FSI is fully confirmed and qualitatively we obtain the same results by the Bochum group [8,9].

5 Summary and perspectives

Recently the inclusive scattering of polarized electrons by a polarized ${}^3\text{He}$ target have been measured at TJLAB, both in the region of the quasi elastic peak and in the low- ω wing. The direct comparison of calculations corresponding to different theoretical approaches with these experimental results allows one to better understand the model dependence in the extraction of the neutron magnetic form factor G_M^n . Indeed for a satisfactory interpretation of the data one needs accurate theoretical calculations that include effects beyond the PWIA, such as i) FSI, ii) MEC, iii) relativistic effects and iv) contributions from the explicit presence of the Δ excitation in the ground state of ${}^3\text{He}$. In our calculations we have adopted both relativistic kinematics and a relativistic electron-nucleon

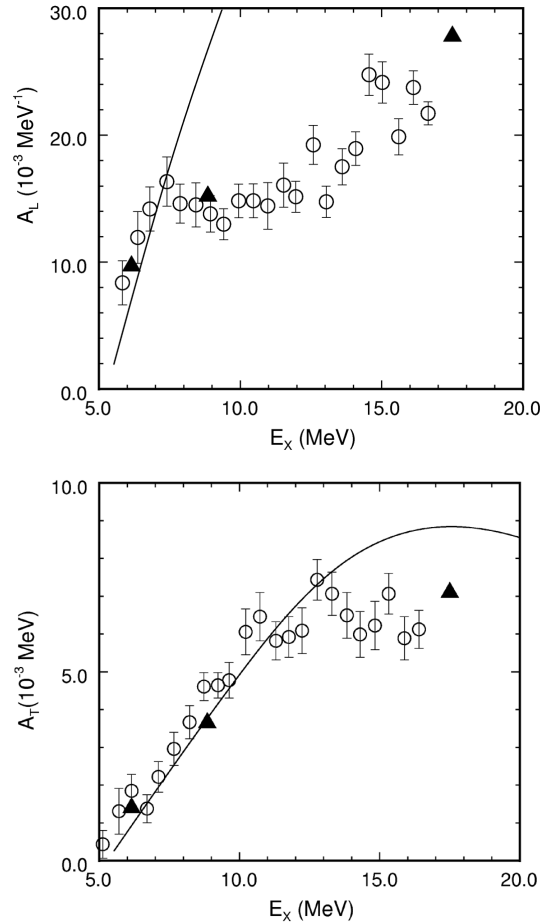


Fig. 6. Unpolarized response functions, A_L and A_T , vs the the missing energy $E_X = \sqrt{(\omega + M_{He})^2 - |\mathbf{q}|^2} - M_{He} \simeq B_3 + \epsilon'_{int}$ for $|\mathbf{q}| \sim 175 \text{ MeV}$. *Solid curves:* PWIA calculations, with unpolarized spectral function obtained [5] from the AV18 nucleon-nucleon interaction [11]. *Triangles:* preliminary calculations with FSI. Experimental data from [18]

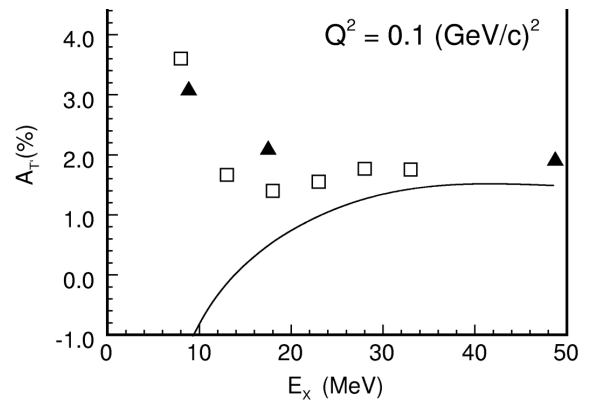


Fig. 7. The transverse response $A_{T'}$ for $Q^2 = 0.1 \text{ (GeV/c)}^2$ vs the excitation energy, E_X , at low transfer, as in Fig. 2. *Solid line:* PWIA; *triangles:* preliminary results with FSI. Experimental data from F. Xiong et al. [14]

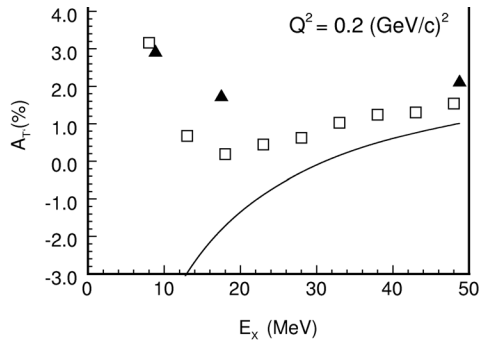


Fig. 8. The same as in Fig. 7, but for $Q^2 = 0.2 \text{ (GeV/c)}^2$

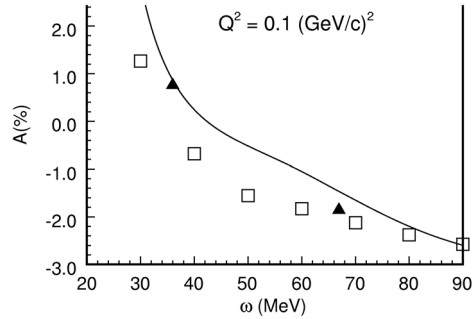


Fig. 9. The transverse response $A_{T'}$ for $Q^2 = 0.1 \text{ (GeV/c)}^2$ vs the energy transfer, ω , in the region of the quasielastic peak. *Solid line:* PWIA; triangles: preliminary results with FSI. Experimental data from W. Xu et al. [10]

cross section [7], and we have taken into account exactly the FSI in the two-body break-up channel, by using the three-nucleon wave functions obtained by the Pisa group [16,17] within a variational approach for both the bound and the excited states.

The development of our approach will follow two distinct paths: i) a better treatment of the relativistic effects

within the so called Relativistic Hamiltonian Dynamics (see, e.g., B.D. Keister and W. Polyzou [19]), that allows a Poincaré covariant description of an interacting system with a fixed number of particles; ii) the inclusion of FSI in the three-body break-up channels, Coulomb effects and three-body forces.

References

1. K. de Jager: e.g. this Conference
2. O. Gayou et al.: Phys. Rev. Lett. **88**, 092301 (2003) and references therein quoted
3. C. Ciofi degli Atti, E. Pace, and G. Salmè: Phys. Rev. C **46**, R1591 (1992)
4. C. Ciofi degli Atti, E. Pace, and G. Salmè, Phys. Rev. C **51**, 1108 (1995)
5. A. Kievsky, E. Pace, G. Salmè, and M. Viviani: Phys. Rev. C **56**, 64 (1997)
6. R.W. Schültze and P.U. Sauer: Phys. Rev. C **48**, 38 (1993)
7. T. De Forest, Jr.: Nucl. Phys. A **392**, 232 (1983)
8. S. Ishikawa, J. Golak, H. Witala, H. Kamada, and W. Glöckle: Phys. Rev. C **57**, 39 (1998)
9. J. Golak, G. Ziemer, H. Kamada, H. Witala, and W. Glöckle: Phys. Rev. C **63**, 034006 (2001)
10. W. Xu et al.: Phys. Rev. Lett. **85**, 2900 (2000)
11. R.B. Wiringa, R.A. Smith, and T.A. Ainsworth: Phys. Rev. C **29**, 1207 (1984)
12. H. Anklin et al.: Phys. Lett. B **428**, 248 (1998)
13. W. Xu et al.: C **67**, 012201 (2003)
14. F. Xiong et al.: Phys. Rev. Lett. **87**, 242501 (2001)
15. G. Kubon et al.: Phys. Lett. B **524**, 26 (2002)
16. A. Kievsky, M. Viviani, and S. Rosati: Phys. Rev. C **64**, 024002 (2001)
17. A. Kievsky, M. Viviani, and S. Rosati: Nucl. Phys. A **577**, 511 (1994)
18. G.A. Retzlaff et al.: Phys. Rev. C **49**, 1263 (1994)
19. B.D. Keister and W.N. Polyzou: Adv. Nucl. Phys. **20**, 225 (1991)